Geozone-Aware Unmanned Aerial Vehicles (UAV) Path Planning Using RRT* and Jellyfish-Inspired Optimization for Urban Air Mobility (UAM)

Judit Salvans Baucells
Industrial Systems Engineering and Product Design
Ghent University
Industrial Systems Engineering (ISyE), FlandersMake@Ugent
Ghent, Belgium
judit.salvansbaucells@ugent.be

Elham Fakhraian
Industrial Systems Engineering and Product Design
Ghent University
Industrial Systems Engineering (ISyE), FlandersMake@Ugent
Ghent, Belgium
elham.fakhraian@ugent.be

Ivana Semanjski
Industrial Systems Engineering and Product Design
Ghent University
Industrial Systems Engineering (ISyE), FlandersMake@Ugent
Ghent, Belgium
ivana.semanjski@ugent.be

Abstract— **The growing demand for autonomous aerial operations highlights the need for efficient and regulation-compliant trajectory planning, particularly in Urban Air Mobility (UAM) applications. This paper presents a UAV path planning framework that combines a geozone-aware Rapidly Exploring Random Tree Star (RRT*) algorithm with a jellyfish-inspired optimization technique to navigate complex airspaces while adhering to safety and regulatory constraints. The method accounts for obstacles, no-fly zones, and altitude limits, and has been tested using real-world geospatial data from Piombino, Italy. Results demonstrate the generation of smooth, efficient trajectories. By enabling scalable and adaptive drone operations, this work supports reliable urban delivery services and integration into future U-space traffic management systems.**

Keywords-Unmanned Aerial Vehicles (UAV); Unmanned Aerial System (UAS); path planning; Rapidly-Exploring Random Tree Star (RRT*); geozones; optimization; jellyfish Swarm algorithm; Urban Air Mobility (UAM).

I. Introduction

Unmanned Aerial Vehicles (UAVs) are playing an increasingly vital role in a wide range of civil applications, including logistics, surveillance, infrastructure inspection, and emergency response. Their growing presence in urban environments brings significant opportunities, but also introduces new challenges related to airspace safety, regulatory compliance, and operational efficiency [1]. To address these concerns, regulatory frameworks have been evolving rapidly. In Europe, the European Union Aviation Safety Agency (EASA) has developed a set of regulations specifically for UAV operations. A key component of this regulatory landscape is the introduction of geozones, which are “portions of airspace where drones, or to use the more official term Unmanned Aerial System (UAS), operations are facilitated, restricted, or excluded” [2]. For example, in urban areas, geozones may prohibit UAV flights over sensitive infrastructure such as airports and government buildings, and restrict altitude near densely populated zones, or define specific aerial corridors above main roads. Adherence to these geozones is mandatory and essential for maintaining safety, minimizing airspace conflicts, and enabling the scalable deployment of UAVs within the broader aviation ecosystem.

Path planning algorithms, particularly sampling-based methods such as Rapidly Exploring Random Trees Star (RRT*), have proven effective in generating feasible trajectories for UAVs in cluttered environments[3]. However, classical RRT* does not inherently account for legal or regulatory constraints. It may produce paths that are kinematically valid but violate geozone boundaries, making them unsuitable for real-world deployment. This paper introduces a geozone-aware extension of the RRT* algorithm that embeds airspace regulatory constraints directly into the path planning process. This enhancement ensures that the generated trajectories are fully compliant with operational regulations. Furthermore, the planning framework incorporates a bio-inspired optimization stage, based on jellyfish swarm behavior, to refine the resulting paths, improving smoothness, efficiency, and safety.

The proposed method is tested using real-world geospatial data from Piombino, Italy, demonstrating its potential to support reliable and scalable UAV operations in regulated urban airspaces. This work contributes to the development of advanced path planning tools essential for the future of UAM and U-space integration in Europe.

Despite its effectiveness, the proposed method relies on static geozone and obstacle data, requiring manual updates when regulations or environments change. It also focuses on single-UAV operations, without yet supporting multi-agent coordination or real-time weather adaptation.

The remainder of this paper is organized as follows: Section 2 reviews related work in UAV path planning and regulatory-aware navigation. Section 3 describes the proposed geozone-aware RRT* framework and the jellyfish-inspired optimization method. Section 4 presents the experimental setup and validation using real-world data from Piombino, Italy. Section 5 discusses the results, including trajectory quality and computational efficiency. Finally, Section 6 concludes the paper and outlines directions for future research.

II. Related Work

Path planning for UAVs has evolved significantly in recent years to meet the demands of increasingly dynamic and constrained airspace. Among various techniques and sampling-based algorithms, particularly RRT and its variant

 ISBN: 978-1-68558-284-5

RRT*, are widely used due to their ability to explore high-dimensional search spaces with low computational cost.

However, the classical version of this methodology has known limitations when applied to real-world operations. It does not account for dynamic constraints or airspace regulations such as altitude ceiling, restricted zones, or geozone boundaries. To address these shortcomings, researchers have proposed a range of extensions to the base algorithm.

Zhang et al. [4] , for example, introduced a potential-based RRT* approach that integrates artificial potential fields into the sampling logic, improving convergence in dense urban areas. In multi-agent scenarios, Li et al. [3] proposed a cooperative bidirectional RRT* framework using potential field heuristics to coordinate multiple UAVs while avoiding conflicts in shared airspace.

Also, hybrid methods have been developed to combine global path generation with local, real-time responsiveness. Himanshu et al. [5] presented an RRT and Velocity Obstacles (VO) structure for Unmanned Traffic Management (UTM), where initial paths are generated offline using RRT, and then refined in real time using VO to avoid dynamic conflicts. Peng et al. [6] extended this idea by incorporating B-spline smoothing to generate continuous, flyable trajectories suitable for UAVs.

In parallel, bio-inspired optimization strategies have been proven to increase effectiveness for post-processing and path selection. Wang et al. [7] proposed a Multi-Objective Jellyfish Search Algorithm (UMOJS) that integrates swarm conduct with adaptive weighting to optimize path length, smoothness, and threat avoidance. While these methods improve flexibility and robustness, they still treat regulatory constraints as a post-processing step. In contrast, our approach integrates geozones awareness directly into the path generation process.

III. METHODOLOGY

The proposed path planning framework, summarized in the workflow diagram on Figure 1, consists of two integrated stages: (1) a geozone-constrained RRT* algorithm that ensures regulation-compliant path generation from the outset, and (2) a jellyfish-inspired stage that selects the best raw trajectory based on multiple objectives and applies smoothing to improve flight stability while preserving regulatory compliance.

A. Geozone-Constrained RRT Expansion*

To ensure that all generated paths are both physically feasible and legally compliant, we extend the standard RRT* algorithm by incorporating regulatory constraints directly into the tree expansion process, ensuring both safety and regulatory compliance, which has been a growing concern in autonomous UAV operations, as highlighted in recent regulatory reviews [8]. Each candidate edge is generated against the following conditions:

- Collision avoidance with 3D environmental obstacles, such as buildings.
- Geozone compliance, ensuring that the edge does not enter prohibited or restricted airspace volumes [2], [9].
- Altitude limits, verifying that flight segments do not exceed the maximum allowable height. typically, 120 meters Above Ground Level (AGL) for civil UAVs in Europe [10], but we restrict our planner to an 80m maximum height and 10m for the minimum limit for a better match with the test scenario characteristics.

Each candidate edge is accepted only if it satisfies all physical and regulatory constraints. This decision process is formalized in equation (1):

$$isValid(e) = \begin{cases} 1, if\ e \cap O = \emptyset,\ e \cap G = \emptyset,\ h(e) \in [h, H] \\ 0, \quad otherwise \end{cases} \tag{1}$$

where e is a candidate edge, O is the set of obstacle volumes, G represents restricted geozones, and $[h, H]$ denotes the edge's altitude range.

If any of these constraints are violated, the edge is rejected from the growing tree. However, instead of passively discarding invalid branches, the planner includes adaptive behaviors aimed at overcoming persistent constraints, unlike methods such as RRT with Velocity Obstacles or spline smoothing, which handle constraints only at post-processing [5][6]. For instance, if a branch consistently encounters a building, the algorithm attempts to reroute above it, provided the new segment remains within legal altitude bounds and moves the UAV closer to its goal.

Regarding the initial and final positions, the planner does not accept arbitrary coordinates. Instead, both start and goal points are randomly selected from a set of physically realistic surfaces. Either ground-level terrain or the rooftops of volumetric structures. If any of the selected start and goal points lie within a restricted geozone, the system first attempts to descend to the nearest collision-free, permitted height. If this is not possible, it searches nearby horizontal positions until such a descent becomes feasible. The horizontal distance allowed within restricted zones during takeoff or landing is strictly limited to ensure regulatory compliance.

To promote flight realism and efficiency, the planner favors stable, horizontal trajectories, maintaining constant altitudes whenever possible. Vertical movements are permitted only when horizontal progress is obstructed. Even in such cases, the algorithm evaluates nearby altitude levels and selects the one with the least obstacle density, balancing safety and flight efficiency.

These three mechanisms, as detailed in Figure 1, operate sequentially and iteratively: constraint-aware expansion ensures initial feasibility, adaptive maneuvering handles repeated constraint conflicts, and temporal validation filters results within a time-bound planning horizon. This combination of constraint-aware expansion, adaptive maneuvering, and temporal validation ensures that all generated trajectories are not only technically feasible but also optimized for legal, safe, and practical deployment in urban airspaces.

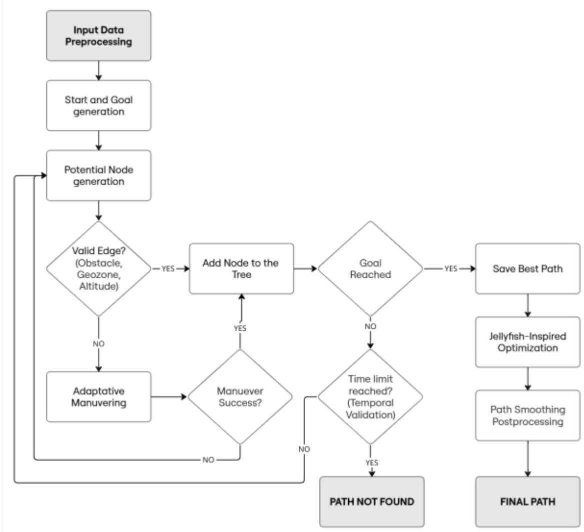

Figure 1. The algorithm's workflow.

B. *Jellyfish-Inspired Optimization*

After generating a set of 10 valid trajectories, the second stage of the framework selects the most suitable one using a lightweight, jellyfish-inspired optimization approach, which has been proven effective in balancing flight criteria [7]. The optimizer, emulating a multi-objective decision-making process, evaluates each candidate path using a composite score derived from three performance metrics:

- Path Length: Total 3D distance traveled, serving as a proxy for energy consumption and mission duration.
- Threat Cost: A cumulative penalty based on proximity to static obstacles, reflecting the overall collision risk.
- Smoothness: Quantified by the sum of angular deviations between consecutive trajectory segments, indicating flight stability and control effort.

All metrics are normalized using min-max scaling to ensure comparability. A randomly sampled weight vector $w = [w_1, w_2, w_3]$, with $\sum_{k=1}^{3} w_k = 1$, is used to compute the composite score for each path i, as presented in the equation (2).

$$Score_i = \sum_{k=1}^{3} w_k \,.\, normalized_{k.i} \tag{2}$$

This stochastic weighting strategy draws inspiration from the adaptive foraging behavior of jellyfish swarms, which adjust their movement patterns in response to environmental stimuli. By sampling different weight combinations for each run, the optimizer implicitly explores diverse trade-offs, sometimes favoring shorter paths, and at other times prioritizing safety or stability. The path with the lowest total score, computed using the randomly sampled weight vectors on all 10 initial simulations, is selected as the final trajectory. This selection mechanism is modular and can easily be extended to incorporate additional criteria, such as estimated energy usage, time-of-day restrictions, or weather-related risk.

In practice, this two-stage approach produces UAV flight paths that are balanced, regulation-compliant, and operationally efficient, making them well-suited for use in real-world UAM scenarios

IV. Case Study: UAV Delivery in Piombino, Italy

To evaluate the effectiveness and real-world applicability of the proposed path planning framework, a comprehensive case study was conducted in Piombino, Italy, as a representative mid-sized coastal city with a mix of residential, industrial, and open areas. The location provides a realistic urban environment with varied terrain, man-made obstacles, and multiple regulatory geozones, making it well-suited for testing UAM planning methods under complex conditions.

A. *Environment and Data Sources*

Terrain elevation data and official geozone definitions were obtained from authoritative sources and national geospatial databases. These datasets were integrated into a 3D simulation environment that reflects Piombino’s actual topography and airspace constraints [9][11].

B. *UAV Specifications*

The UAV simulated in this study is based on the commercially available multirotor platform DJI Matrice 300 RTK, shown in Figure 2. This model was selected because of its size, weight, and flight characteristics, detailed in Table I, are suitable for typical urban applications such as parcel or medical delivery. Its specifications defined the applicable regulatory context, under EASA’s Open Category A3, which imposes specific restrictions on flight altitude, proximity to people, and operational environments [10].

Also, the working temperature range aligns with local conditions in Piombino, and its maximum speed and flight time allow it to cover up to 75.9 kilometers, which is more than sufficient for the scale of the study area. While these specifications are not directly integrated into the path-planning algorithm as constraints, they serve to ground the case study in a realistic operational and regulatory context. This ensures that the mission profiles and legal framework used in the simulation reflect real-world deployments, while also supporting potential future extensions such as energy-aware planning or charging station integration.

Figure 2. DJI Matrice 300 RTK [12].

TABLE I. THE DJI MATRICE 300 RTK MAIN SPECIFICATIONS [12].

Parameter	*Value*
Max Payload	3.6 kg
Max Flight Time	55 min
Max Speed	23 m/s
Operating Temperature	-20ºC to 50ºC

C. Mission Scenarios

A total of sixteen diverse origin-destination pairs were randomly defined across the study area to ensure broad coverage of different locations, obstacle densities, and geozone configurations. Although all scenarios are set within the same urban environment, the variation in spatial layouts allows the planner to be tested under diverse conditions. The complete list of origin-destination pairs is provided in Table II. Each pair was executed 10 times per configuration to assess its robustness and consistency. Consistent success rates and stable path quality metrics (e.g., length, smoothness, and threat cost) across runs indicate the planner's reliability.

TABLE II. ORIGIN-DESTINATION PAIRS.

Nº	Start			Goal		
	Lon	Lat	Alt	Lon	Lat	Alt
A	10.5375	42.9361	30.9	10.5313	42.9310	22.7
B	10.5350	42.9307	25.2	10.5335	42.9295	0.5
C	10.5326	42.9330	27.7	10.5301	42.9320	22.9
D	10.5360	42.9308	29.5	10.5377	42.9376	20.5
E	10.5318	42.9305	0.5	10.5393	42.9363	0.5
F	10.5354	42.9356	31.4	10.5364	42.9308	25.4
G	10.5332	42.9303	32.1	10.5384	42.9339	0.5
H	10.5398	42.9298	0.5	10.5314	42.9289	34.4
I	10.5363	42.9293	21.5	10.5336	42.9349	28.4
J	10.5381	42.9345	30.6	10.5327	42.9329	0.5
K	10.5353	42.9292	0.5	10.5333	42.9320	0.5
L	10.5335	42.9289	40.9	10.5296	42.9288	26.1
M	10.5339	42.9343	0.5	10.5399	42.9261	0.5
N	10.5320	42.9301	0.5	10.5334	42.9303	32.1
O	10.5375	42.9361	30.9	10.5377	42.9296	28.1
P	10.5358	42.9369	23.3	10.5374	42.9308	25.7

V. RESULTS

To assess the performance and adaptability of the proposed UAV path planning framework, we conducted a series of experiments focusing on the impact of varying the STEP_SIZE parameter during RRT* tree expansion. This parameter determines the incremental distance between nodes and plays a critical role in balancing solution quality, computational cost, and planning success.

A. Parameter Evaluation: STEP_SIZE Impact

Four values of STEP_SIZE (4, 8, 12, and 14 meters) were tested across all origin-destination pairs. These values were selected based on early development insights: smaller steps improved the path significantly, increased execution time, while larger steps sped up computation but reduced success rates. Also, step sizes larger than 14 meters were not considered in the final evaluation because they sometimes caused the planner to miss narrow obstacles, slipping over them without proper detection due to the coarse sampling resolution. Finally, a time limit of 250 seconds was set for each run to keep computation times within practical bounds.

Table III summarizes the average performance across all metrics for each tested STEP_SIZE, based on multiple executions of each configuration. The evaluation metrics included are:

- Success Rate (%): Percentage of runs that resulted in valid, regulation-compliant paths.
- Execution Time (s): Average computation time required to generate a trajectory.
- Path Length: Total 3D distance of the trajectory.
- Threat Cost: Cumulative penalty for proximity to obstacles, indicating environmental risk.
- Smoothness: Sum of angular deviations between consecutive path segments.
- Node Count: Average number of RRT* nodes required to construct the path.

TABLE III. IMPACT OF STEP_SIZE ON PERFORMANCE.

Metric	4	8	10	12	14
Success Rate (%)	40.0	70.62	71.88	79.38	77.5
Execution Time (s)	68.06	45.22	43.55	24.81	25.26
Path Length	4.34*	4.02*	4.0*	4.22*	4.07*
Threat Cost	2.67*	1.32*	0.96*	0.69*	0.6*
Node Count	2.01*	2.01*	1.62*	1.71*	1.39*
Smoothness	6.15*	3.16*	2.64*	2.42*	2.03*

B. Path Smoothing and Postprocessing

RRT*- based paths, though feasible, often include abrupt angular changes or minor detours that can degrade flight stability, increase energy consumption, and challenge onboard autopilot systems, a limitation also noted in prior RRT*- based planning studies [13]. To address this, we applied a postprocessing smoothing algorithm designed to enhance path fluidity while preserving legality. The smoothing process uses a sliding window averaging filter: each waypoint is adjusted based on the average position of its immediate neighbors, effectively reducing sharp transitions. To ensure regulatory compliance, each smoothed waypoint is validated against all constraints (e.g., geozone boundaries, altitude limits, and obstacle collisions). If a violation is detected, the point is reverted to its original position.

Post-smoothing, the trajectory's smoothness metric is re-evaluated, typically revealing significant improvements with negligible changes in path length or threat exposure. This enhancement contributes to more energy-efficient and dynamically stable UAV flights. Figure 3 illustrates this process on a representative example, Experiment D, corresponding to the start and goal points listed as pair D in Table II. The raw trajectory - Figure 3(a) exhibits several unnecessary turns and sharper angles, while the smoothed version - Figure 3(b) shows a more direct and stable path towards the destination, offering more realistic and controllable flight behavior.

a)

b)

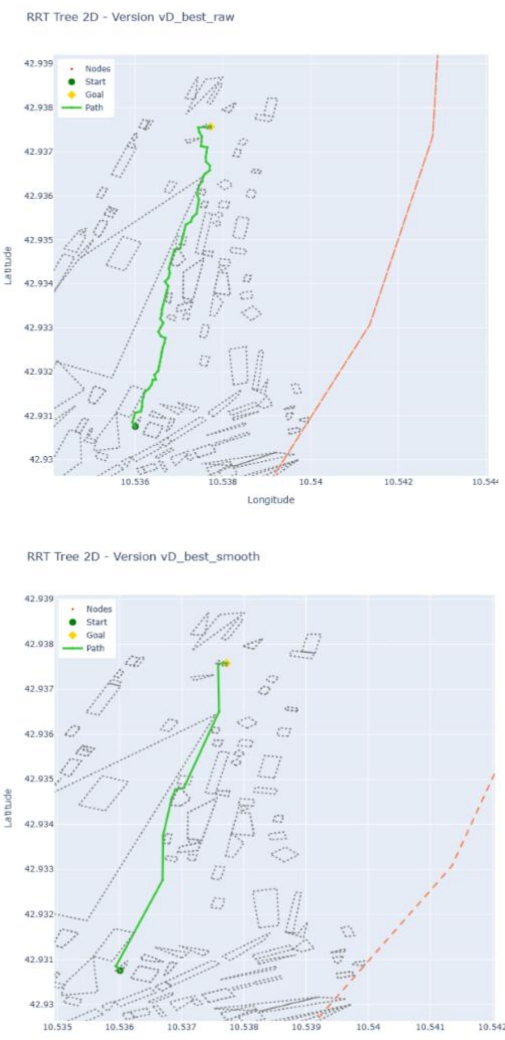

Figure 3. Trajectory Comparison between (a) initial RRT* path and (b) postprocessed trajectory.

C. Optimization Results

The jellyfish-inspired optimizer was used to select the best trajectory among 10 valid candidates for each mission scenario. Based on a composite score, combining path length, smoothness, and threat cost with randomly sampled weights, the optimizer prioritized balanced paths without additional computational cost. In all test cases, the selected trajectories already demonstrated better overall quality than the raw alternatives. After selection, a lightweight smoothing process is applied to further enhance flight realism by reducing sharp turns. This step preserved all regulatory constraints while improving the trajectory's fluidity and controllability, both assessed using the smoothness metric, based on angular deviations between path segments, which indirectly evaluates the presence of abrupt transitions.

Together, the optimization and smoothing stages significantly improved the final path quality, enabling safe, efficient, and realistic UAV operations in constrained urban environments.

D. Geozone-Aware Path Planning Result

A key objective of the proposed algorithm is to ensure that all trajectories remain fully compliant with regulatory geozone constraints. The geozone-aware RRT* planner achieves this by filtering geospatial violations during node expansion and enforcing strict exclusion of restricted volumes throughout the trajectory. The only permitted geozones entry occurs during the initial takeoff or final descent.

Figure 4(a) provides a clear example of this behavior, taken from experiment D. In this case, the UAV has the start point inside a restricted geozone and performs a vertical descent to reach a valid flight altitude before continuing horizontally toward the destination. Conversely, Figure 4(b) shows the trajectory from experiment E, where neither the start nor the goal lies within a restricted zone. And the final example is in Figure 4(c), where both the start and the goal points are inside the restricted volumes of the geozones. The comparison demonstrates the planner's adaptability to different constraints or situations.

Overall, across all scenarios, the planner successfully generated paths that respected all airspace regulations, maintaining safety and legality even in dense and constrained urban environments.

VI. Discussion

The proposed path planning methodology demonstrates a robust ability to generate compliant geozones, obstacle-free UAV trajectories across a wide variety of urban conditions. The combination of the regulation-aware RRT* expansion with the multi-objective trajectory selection and the final smoothness postprocess results in a consistent, safe, and efficient performance. Results across all 16 mission scenarios show that the algorithm can adapt to various obstacle densities and regulatory constraints.

However, the performance variations observed across different configurations suggest that some mission scenarios are inherently more complex. This is likely due to the spatial arrangement of certain origin-destination pairs, the proximity of restricted zones, or the presence of specific obstacles that hinder maneuverability. These findings highlight the importance of introducing more refined and context-aware constraints when defining operational areas.

The methodology also presents some structural limitations. It relies on static representations of geozones and environmental obstacles, requiring manual updates to reflect changes in airspace regulations or urban infrastructure.

Nonetheless, once the input data is updated, the algorithm is fully capable of recalculating optimized trajectories under new conditions without requiring internal modifications. This highlights its adaptability to different urban scenarios and regulatory environments, provided that accurate and up-to-date inputs are supplied. Moreover, as currently implemented, the system assumes a single-UAV context and does not incorporate weather conditions, which may influence practical deployment feasibility in complex environments.

a) b) c)

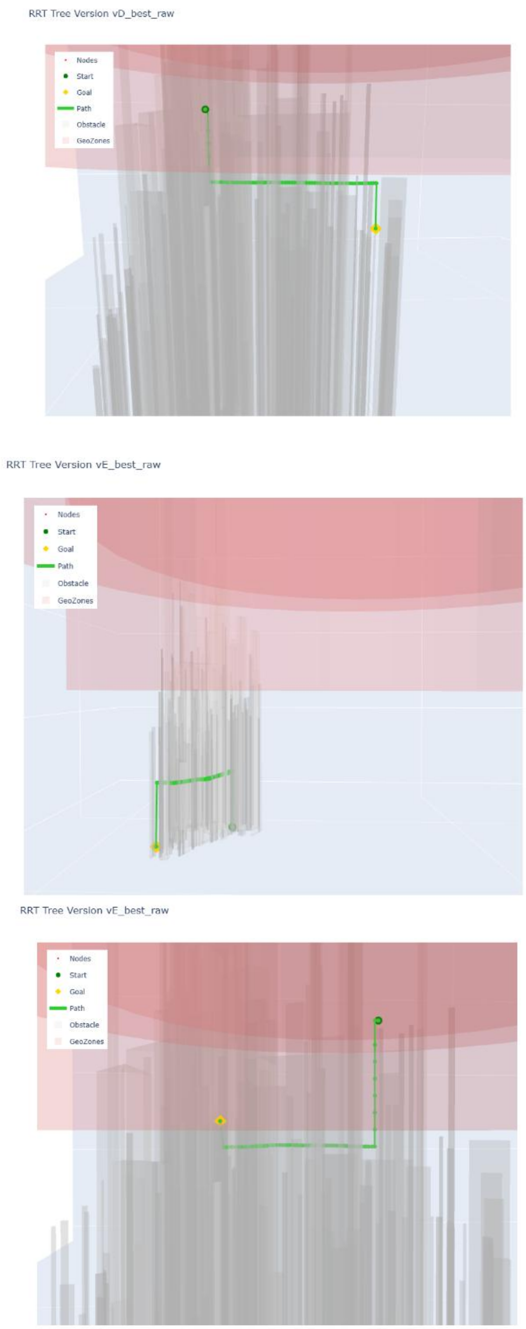

Figure 4. Trajectory Comparison between (a) example of geozone-aware vertical geozone avoidance, (b) example of a path without geozones interference, and (c) example of a path with start and goal points inside a geozone.

VII. CONCLUSION AND FUTURE WORK

This work introduces a UAV path planning strategy that respects both physical and regulatory constraints in urban airspace. By combining a geozone-aware RRT* with a lightweight, jellyfish-inspired optimizer, the system generates safe, efficient, and regulation-compliant trajectories. Tested on real-world data, the planner delivered consistent results while maintaining low computational demand and requiring only lightweight postprocessing. Specifically, the path generation times remained within practical limits, and the postprocessing stage, focused on smoothing and basic filtering, was kept simple, without relying on heavy optimization frameworks or complex interpolation techniques.

As future work, we aim to analyze which specific areas of the urban environment systematically reduce planning success or limit trajectory feasibility. Identifying such "critical areas" could help make operational decisions, such as excluding them from permitted takeoff or landing locations or avoiding them as candidate sites for drone charging stations. This geospatial analysis would support more reliable UAV operations by guiding the placement of more infrastructure and enabling smarter regulation-aware launch and recovery strategies. In parallel, incorporating dynamic geozone updates via real-time regulatory feeds or U-space integration could further enhance the system's adaptability to temporary restrictions and evolving airspace conditions.

Another future direction involves enabling multi-UAV coordination under shared constraints, especially in scenarios like medical supply distribution or emergency evacuation. This may require a centralized coordination layer or negotiation protocols. Additionally, temporary regulations issued during events like wildfires or floods could be incorporated through real-time updates from civil authorities or firefighting services

ACKNOWLEDGMENT

This work was supported by the funding from the European Union's Horizon 2020 research and innovation program under grant agreement No 101007134 and Regional and community funding: Special Research Fund's project Robust and Trustworthy Smart Mobility Systems (grant number BOF/STA/202209/004).

REFERENCES

[1] E. Fakhraian, I. Semanjski, S. Semanjski, and E. H. Aghezzaf, "Towards Safe and Efficient Unmanned Aircraft System Operations: Literature Review of Digital Twins' Applications and European Union Regulatory Compliance," Jul. 01, 2023, Multidisciplinary Digital Publishing Institute (MDPI). doi: 10.3390/drones7070478.

[2] European Union Aviation Safety Agency (EASA), "Geo-Zones – know where to fly your drone." Accessed: Jan. 20, 2025. [Online]. Available: https://www.easa.europa.eu/en/light/topics/geo-zones-know-where-fly-your-drone#:~:text=Geo%2Dzones%20are%20portions%20of,protect%20the%20privacy%20of%20others

[3] C. Wu, Z. Guo, J. Zhang, K. Mao, and D. Luo, "Cooperative Path Planning for Multiple UAVs Based on APF B-RRT*

 ISBN: 978-1-68558-284-5

Algorithm," *Drones*, vol. 9, no. 3, Mar. 2025, doi: 10.3390/drones9030177.

[4] X. Xu, F. Zhang, and Y. Zhao, "Unmanned Aerial Vehicle Path-Planning Method Based on Improved P-RRT* Algorithm," *Electronics (Switzerland)*, vol. 12, no. 22, Nov. 2023, doi: 10.3390/electronics12224576.

[5] Himanshu, J. V. Pushpangathan, and H. Kandath, "RRT and Velocity Obstacles-based motion planning for Unmanned Aircraft Systems Traffic Management (UTM)," Feb. 2023, [Online]. Available: http://arxiv.org/abs/2302.14543

[6] M. Peng and W. Meng, "Cooperative Obstacle Avoidance for Multiple UAVs Using Spline_VO Method," *Sensors*, vol. 22, no. 5, Mar. 2022, doi: 10.3390/s22051947.

[7] X. Wang, Y. Feng, J. Tang, Z. Dai, and W. Zhao, "A UAV path planning method based on the framework of multi-objective jellyfish search algorithm," *Sci Rep*, vol. 14, no. 1, Dec. 2024, doi: 10.1038/s41598-024-79323-0.

[8] E. Fakhraian, I. Semanjski, S. Semanjski, and E. H. Aghezzaf, "Towards Safe and Efficient Unmanned Aircraft System Operations: Literature Review of Digital Twins' Applications and European Union Regulatory Compliance," Jul. 01, 2023, *Multidisciplinary Digital Publishing Institute (MDPI)*. doi: 10.3390/drones7070478.

[9] d-flight, "Italian u-space platform." Accessed: Jun. 02, 2025. [Online]. Available: https://www.d-flight.it/web-app/

[10] European Union Aviation Safety Agency (EASA), "Open Category of Civil Drones." Accessed: Feb. 01, 2023. [Online]. Available: https://www.easa.europa.eu/domains/civil-drones/drones-regulatory-framework-background/open-category-civil-drones

[11] Regione Toscana, "Geoscopio." Accessed: Jun. 02, 2025. [Online]. Available: https://www.regione.toscana.it/-/geoscopio

[12] DJI, "Matrice 300 rtk specifications." Accessed: Jun. 02, 2025. [Online]. Available: https://www.dji.com/be/support/product/matrice-300

[13] H. Li, R. Jia, Z. Zheng, and M. Li, "Energy-Efficient UAV Trajectory Design and Velocity Control for Visual Coverage of Terrestrial Regions," *Drones*, vol. 9, no. 5, May 2025, doi: 10.3390/drones9050339.